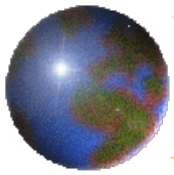


# Response of terrestrial aridity to global warming

Qiang Fu

Department of Atmospheric Sciences

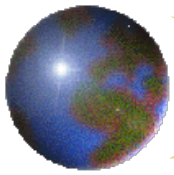
University of Washington



# Introduction

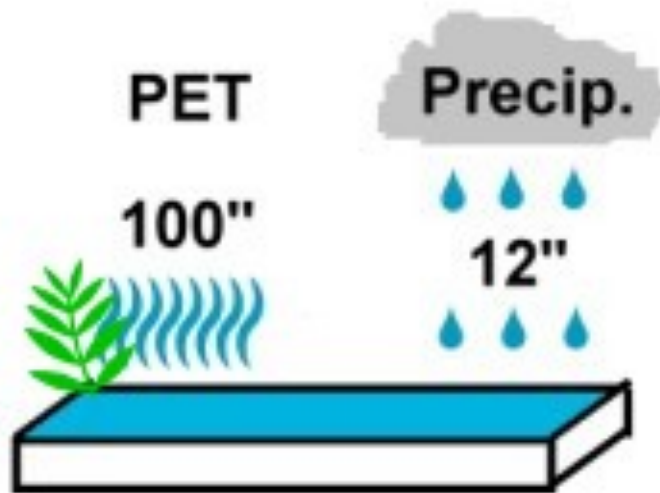


- Potential evapotranspiration ( $PET$ ): The maximum amount of water capable of being lost from the surface for given atmospheric condition with well supplied surface water (i.e., the evaporative demand of the atmosphere).

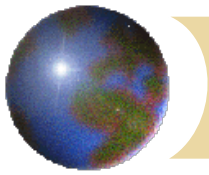


- ✚ Aridity index (UNEP 1992):

$$AI = P/PET$$



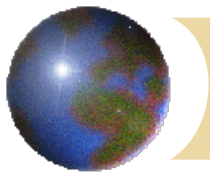
e.g., at Tucson, USA  
 $P/PET = 0.12$



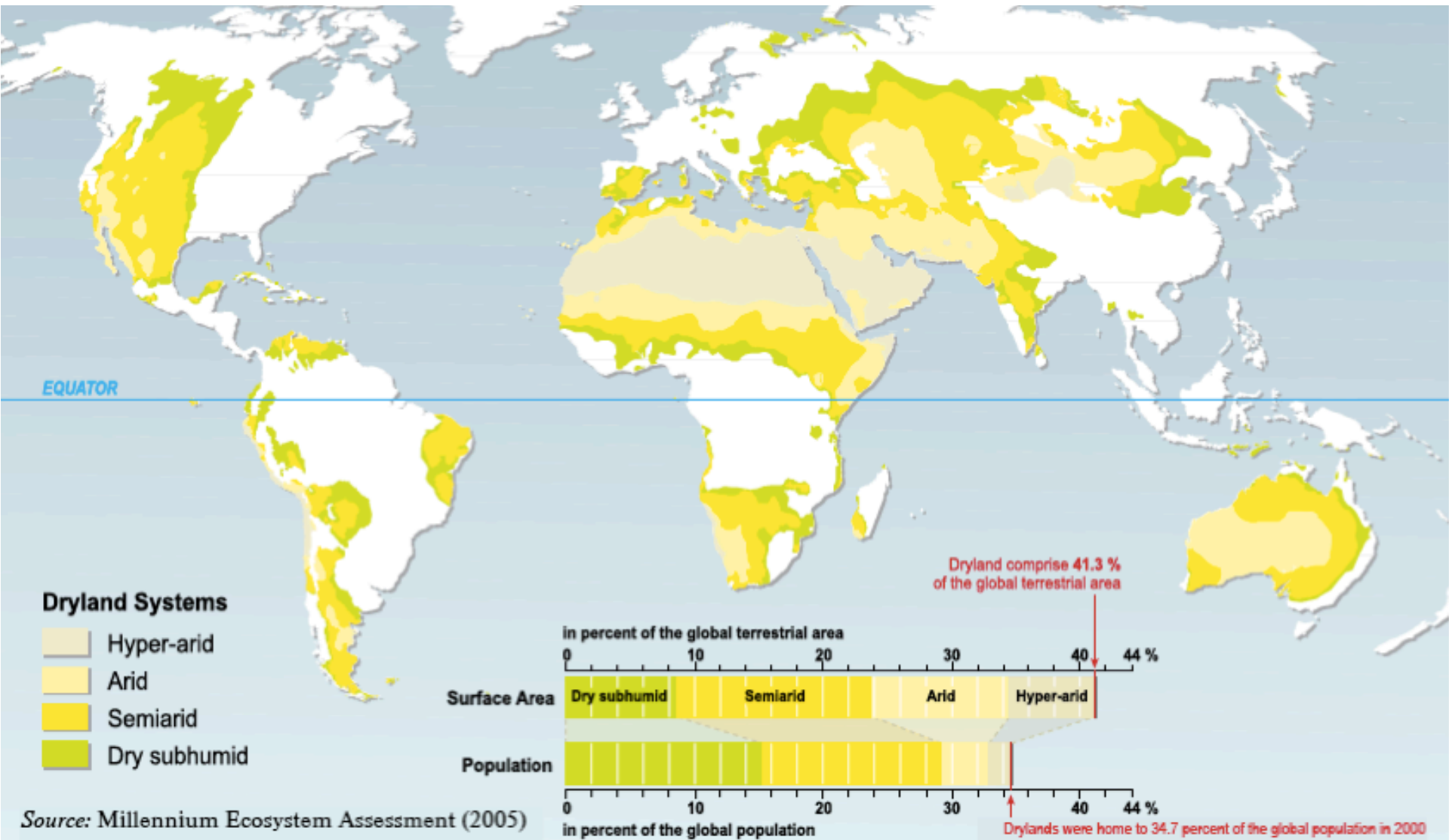
• Drylands are regions with  $P/PET < 0.65$ , which are further divided into (UNEP 1992; Hulme 1992):

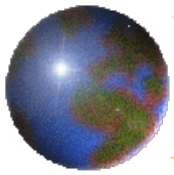
- Hyper-arid:  $P/PET < 0.05$
- Arid:  $0.05 < P/PET < 0.20$
- Semid-arid:  $0.20 < P/PET < 0.50$
- Dry subhumid:  $0.50 < P/PET < 0.65$





# Distribution of World's Drylands

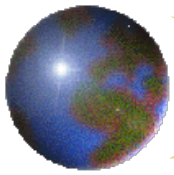




- How does terrestrial aridity in terms of  $P/PET$  respond to anthropogenic climate change?



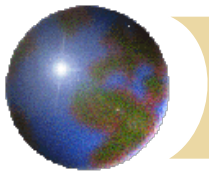
A view of dryland (with village in the background) in the Sahel, southern Niger



- Previous studies focus on change in precipitation, as typical in high-profile reports (e.g., [IPCC 2007, 2014](#)), which may not tell the whole story – or perhaps even the main story – of hydrological change.



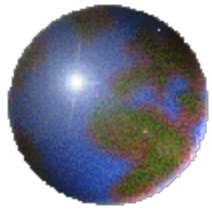




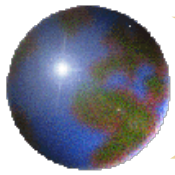
- ✚ Most studies of terrestrial dryness focus on droughts (e.g., Dai 2013), rather than on the background aridity changes.



- ✚ Drought region versus arid region
  - Anomaly (extreme) versus mean state (background climatology)

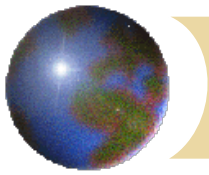


- Introduction
- A drier terrestrial climate
  - Global dryland expansion
- Past, present, and future
- Conclusions



## • A drier terrestrial climate

- Observational data for 1948-2010
  - $T$  and  $P$ : CPC and UD
  - $R$ ,  $RH$  and  $u$ : GLDAS and the 20<sup>th</sup> Century Reanalysis
- Model data for 1948-2100
  - 27 CMIP5 GCMs with historical forcings for 1948-2005 and RCPs 8.5 and 4.5 for 2006-2100
  - The simulated data were statistically downscaled to 0.5 degree resolution
- CMIP5 transient  $\text{CO}_2$  1%/yr increase experiments
  - 25 CMIP5 GCMs to doubling  $\text{CO}_2$

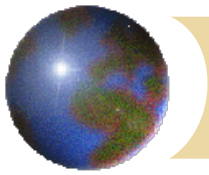


## • *PET* algorithm

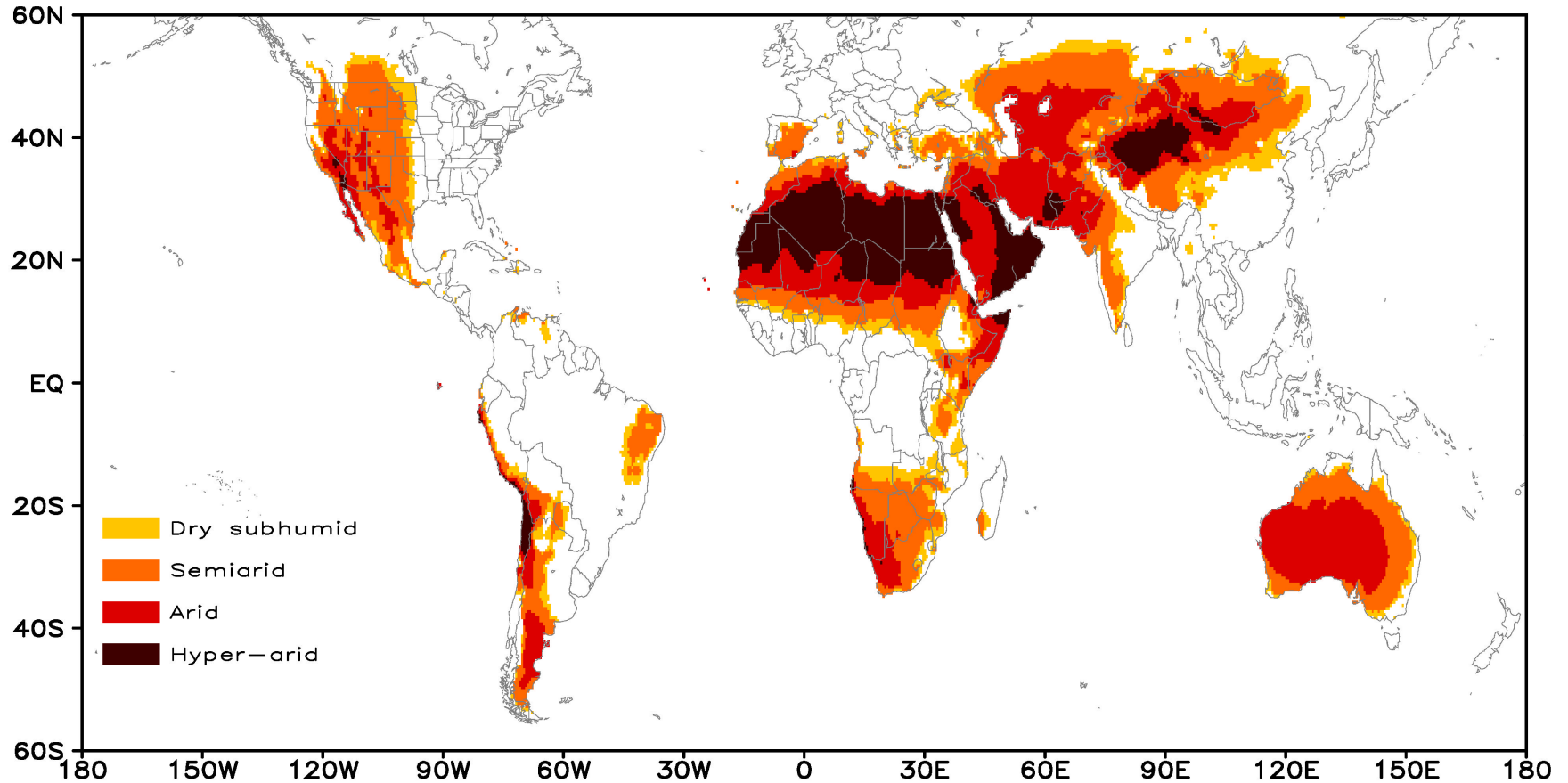
- The *PET* is based on the Penman-Monteith (PM) algorithm (Maidment 1993; Allen et al. 1998; Sheffield et al. 2012; Scheff & Frierson 2014):

$$PET = \frac{(R_n - G)\Delta(T_a) + \rho_a c_p e^*(T_a)(1 - RH)C_H |u|}{\Delta(T_a) + \gamma(1 + r_s C_H |u|)} / L_v$$

where  $R_n - G$  is the surface available energy,  $T_a$  temperature,  $RH$  relative humidity, and  $u$  wind;  $e^*$  is saturated water vapor pressure,  $\Delta = de^*/dT$ ,  $C_H$  transfer coefficient ( $4.8 \times 10^{-3}$ ),  $r_s$  bulk stomatal resistance under well-water conditions (70 s/m).

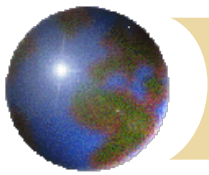


## Global dryland distribution for 1961-1990 climatology

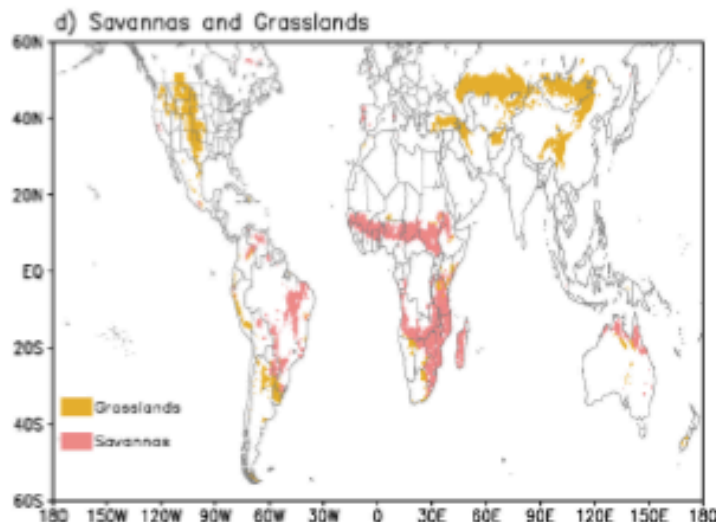
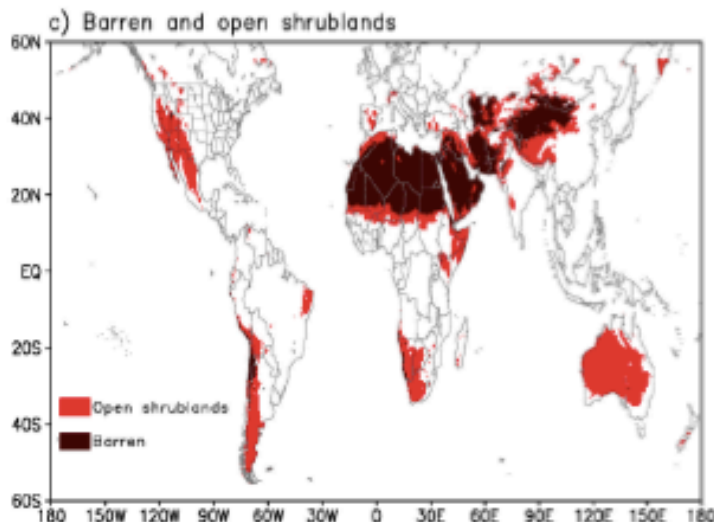
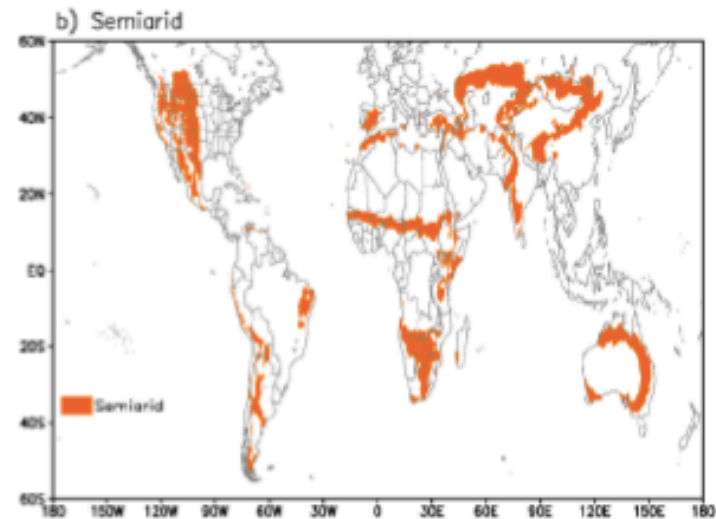
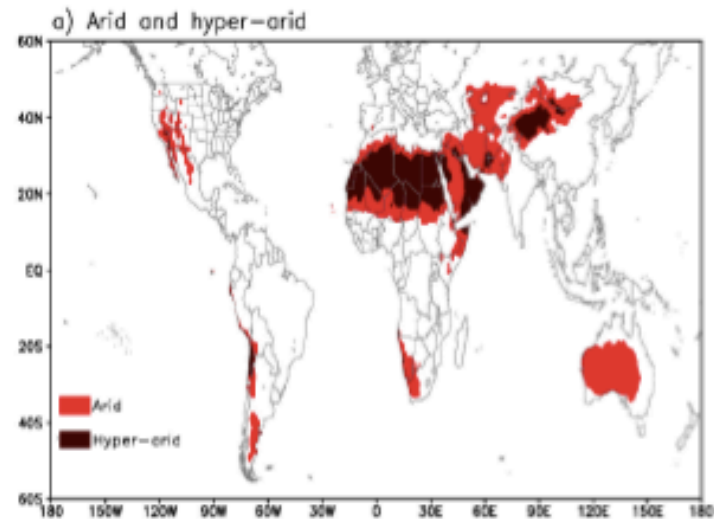


Feng & Fu (2013)

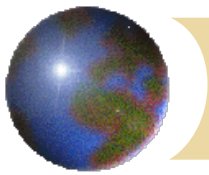




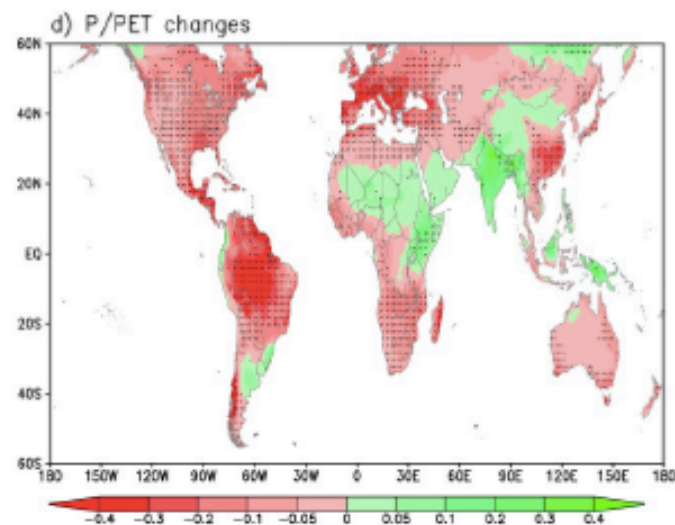
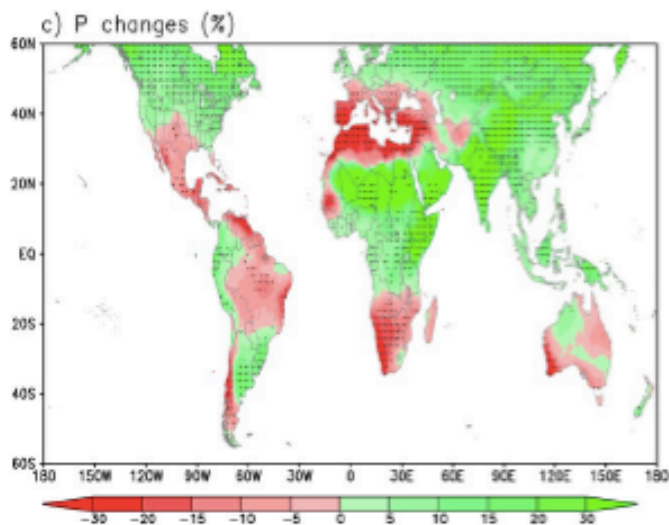
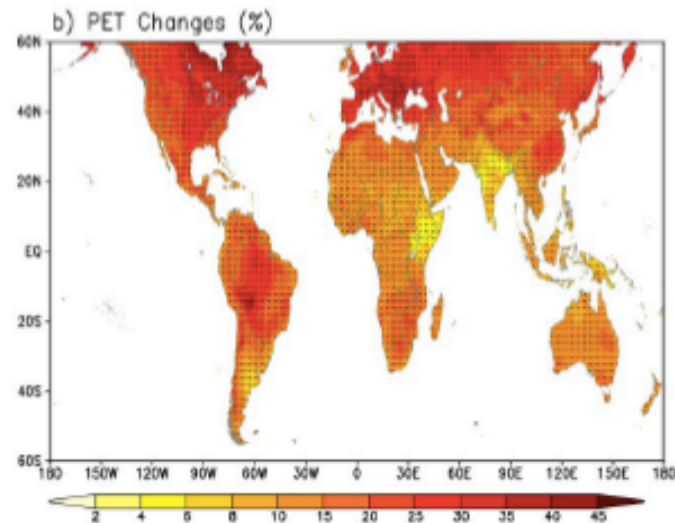
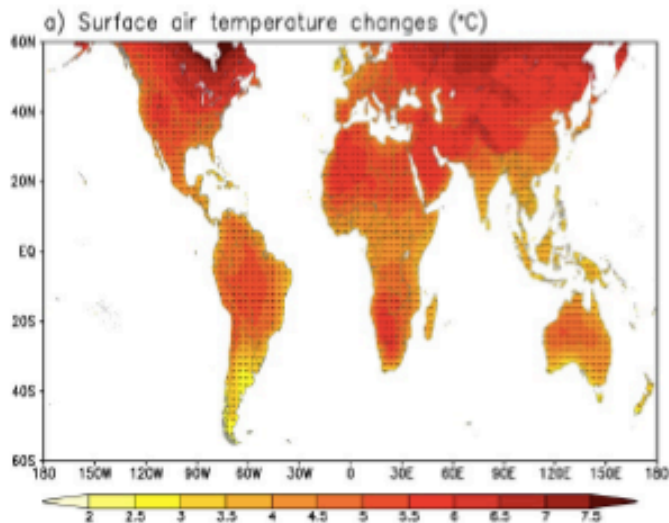
# Global dryland distributions versus vegetation types from MODIS



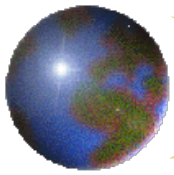
Feng & Fu  
(2013)



Changes in (a) surface air temperature, (b)  $PET$ , (c) precipitation, and (d)  $P/PET$  (1961-1990 to 2071-2100) under scenario RCP85

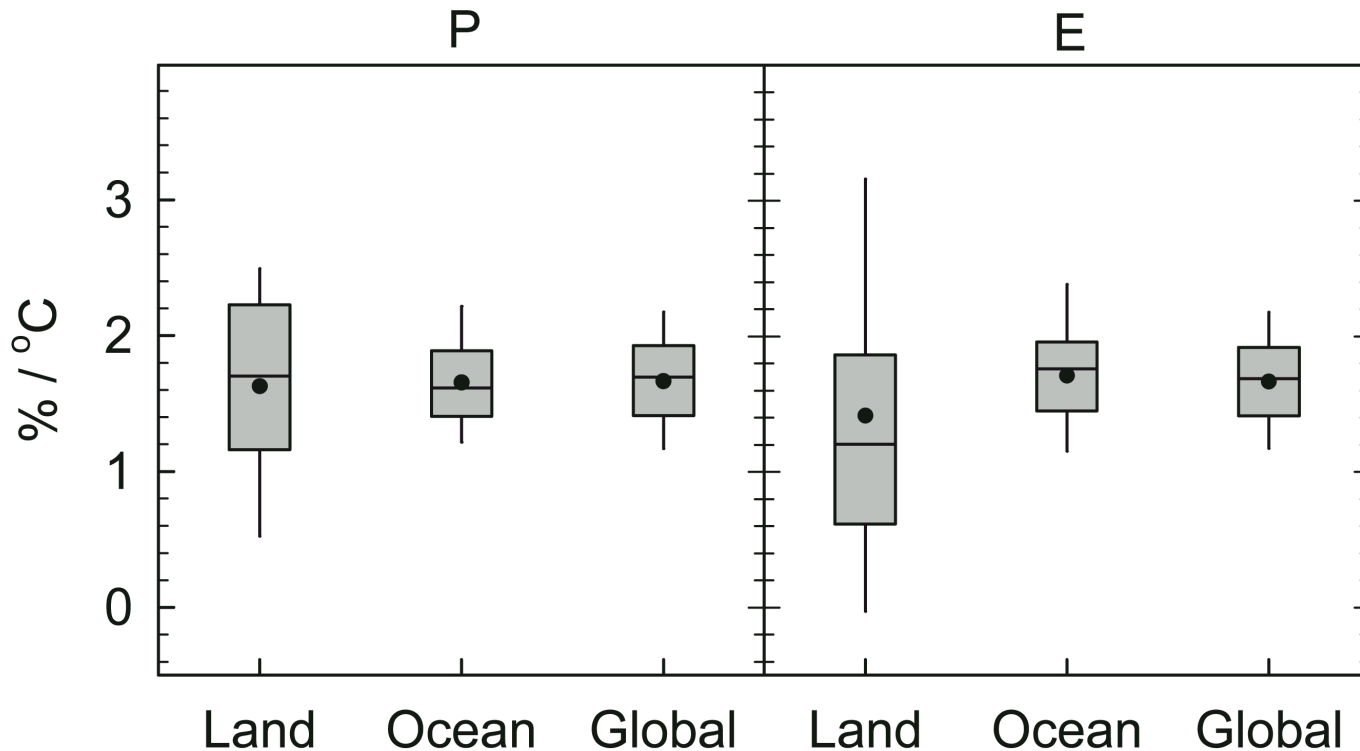


Feng & Fu  
(2013)

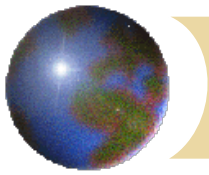


## Why do we expect a drier climate under global warming

- As the globe warms global average rainfall increases (e.g., Allen and Ingram, 2002).



Fu & Feng  
(2014)

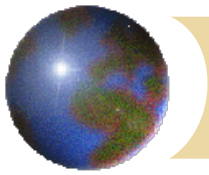


The percentage change in  $P/PET$  can be written as

$$\Delta\left(\frac{P}{PET}\right) / \left(\frac{P}{PET}\right) \approx \frac{\Delta P}{P} - \frac{\Delta PET}{PET}$$

Noting a similar rate of percentage increase in  $P$  over land to that in  $E$  over ocean, we have

$$\Delta\left(\frac{P}{PET}\right) / \left(\frac{P}{PET}\right) \approx \left(\frac{\Delta E}{E}\right)_{Ocean} - \frac{\Delta PET}{PET}$$



- The Penman-Monteith algorithm can be used to estimate the actual  $E$  over ocean by setting  $r_s = 0$  and using a  $C_H$  of  $1.5 \times 10^{-3}$  (Richter and Xie 2008), i.e.,

$$E = \frac{(R_n - G)\Delta(T_a) + \rho_a c_p e^*(T_a)(1 - RH)C_H |u|}{\Delta(T_a) + \gamma} / L_v$$

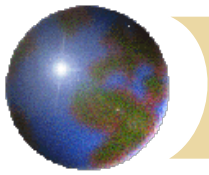
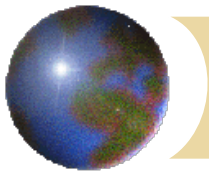


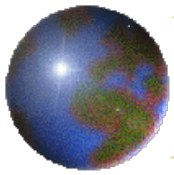
Table. Comparison of annual mean evaporation ( $E$ ) and its percentage change rate and surface stability ( $T_a - T_s$ ) change rate over ocean estimated using the PM algorithm and those from the GCMs.

	$E$ (mm)	Percentage change rate in $E$ (%/°C)	Change rate in $T_a - T_s$ (°C/°C)
<i>Penman-Monteith</i>	1267 (90)	1.92 (0.39)	0.07 (0.03)
<i>Directly from GCMs</i>	1300 (62)	1.71 (0.40)	0.06 (0.02)

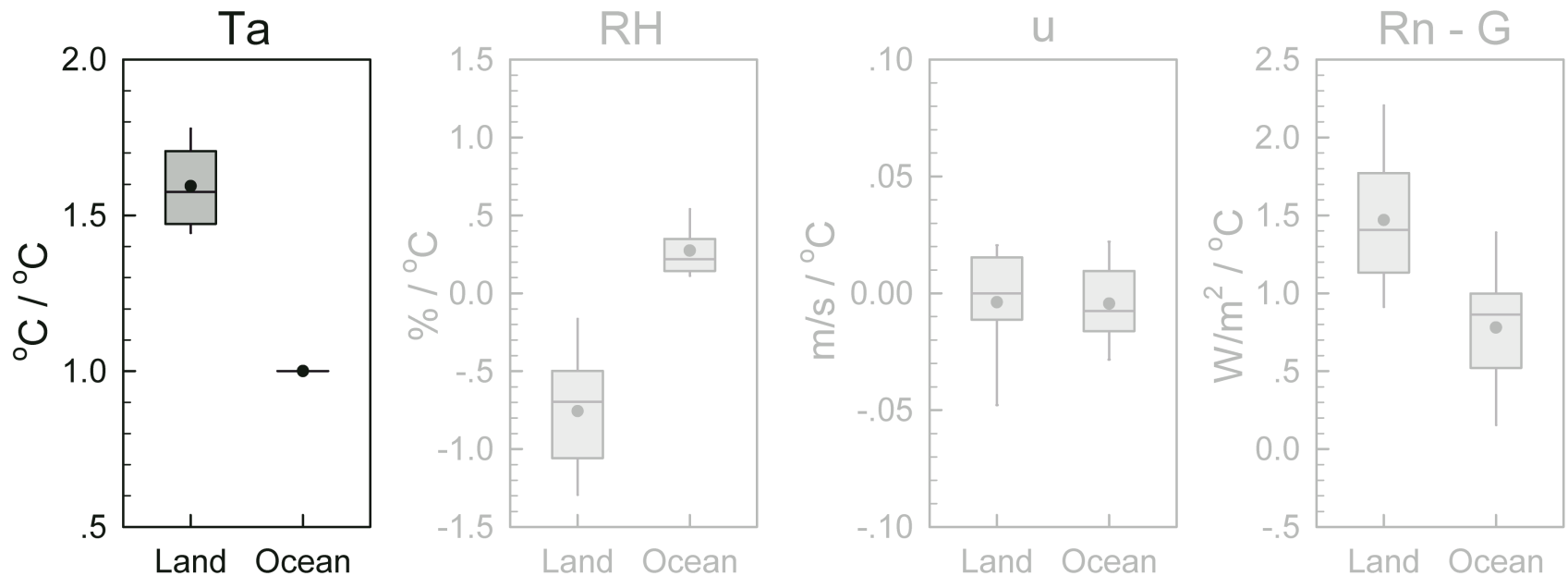
Fu & Feng (2014)



- ✚ Since the PM algorithm can be applied to both  $PET$  over land and  $E$  over ocean, we can examine the change in  $P/PET$  in the framework of the  $PET$  by comparing its changes over land and ocean.
- ✚ Both  $PET$  over land and  $E$  over ocean are a function of surface air temperature ( $T_a$ ), relative humidity ( $RH$ ), wind speed ( $u$ ), and available energy ( $R_n - G$ ).

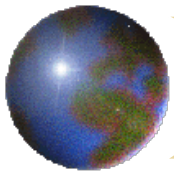


- Ingredient one: Land surface warms on average, about 50% more than oceans (e.g., Manabe et al. 1992; Joshi et al. 2008)

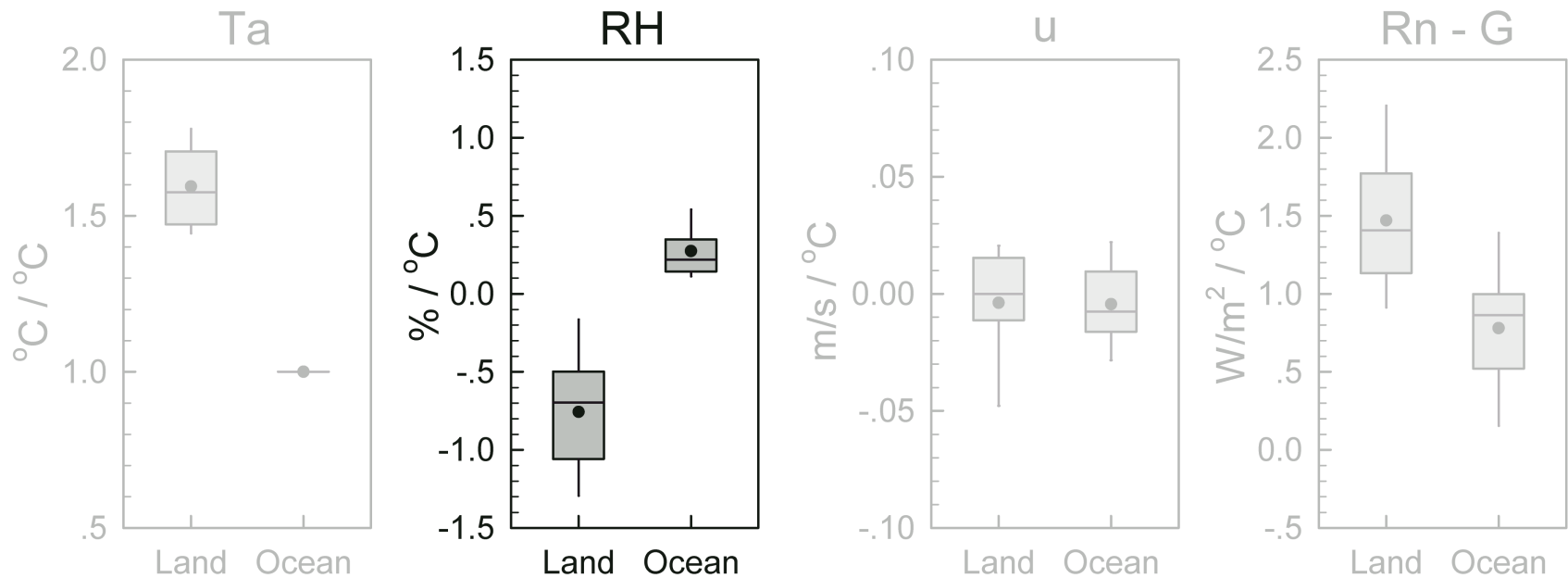


Fu & Feng (2014)

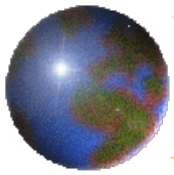




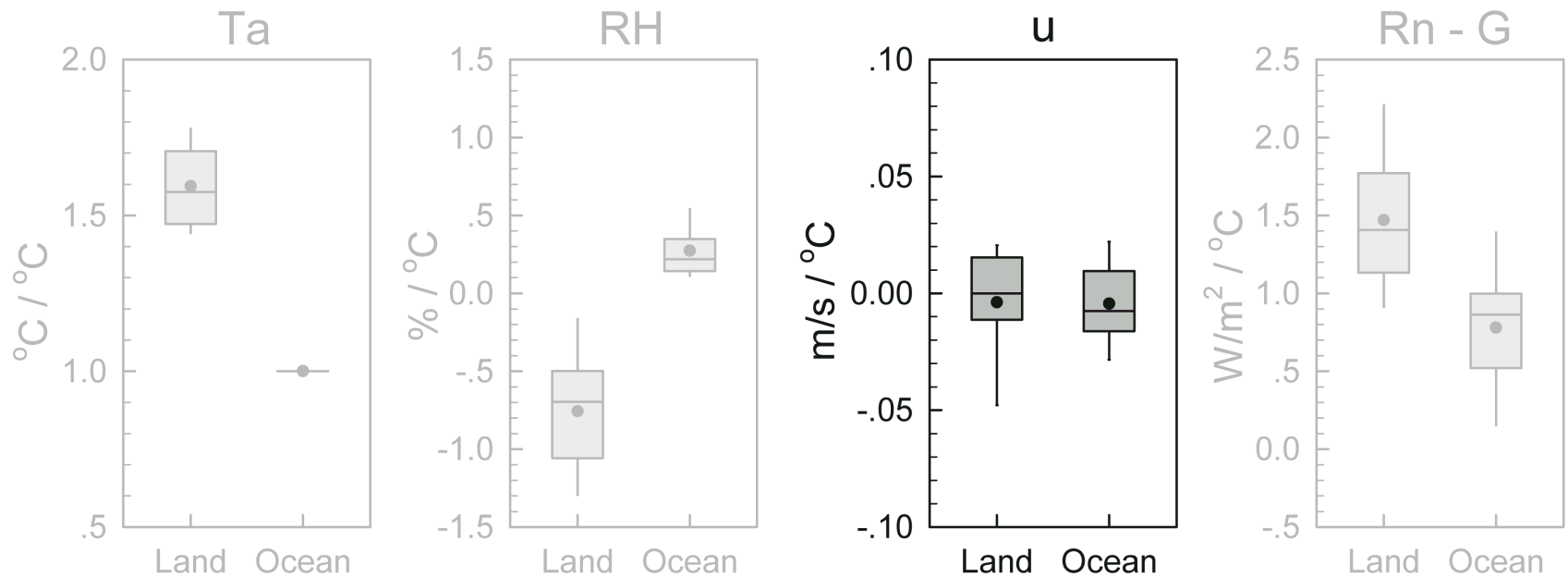
- Ingredient two: Reduced relative humidity near the surface over land but increased RH over ocean (e.g., Simmons et al. 2010; O’Gorman and Muller 2010; Sherwood and Fu 2014)



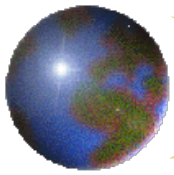
Fu & Feng (2014)



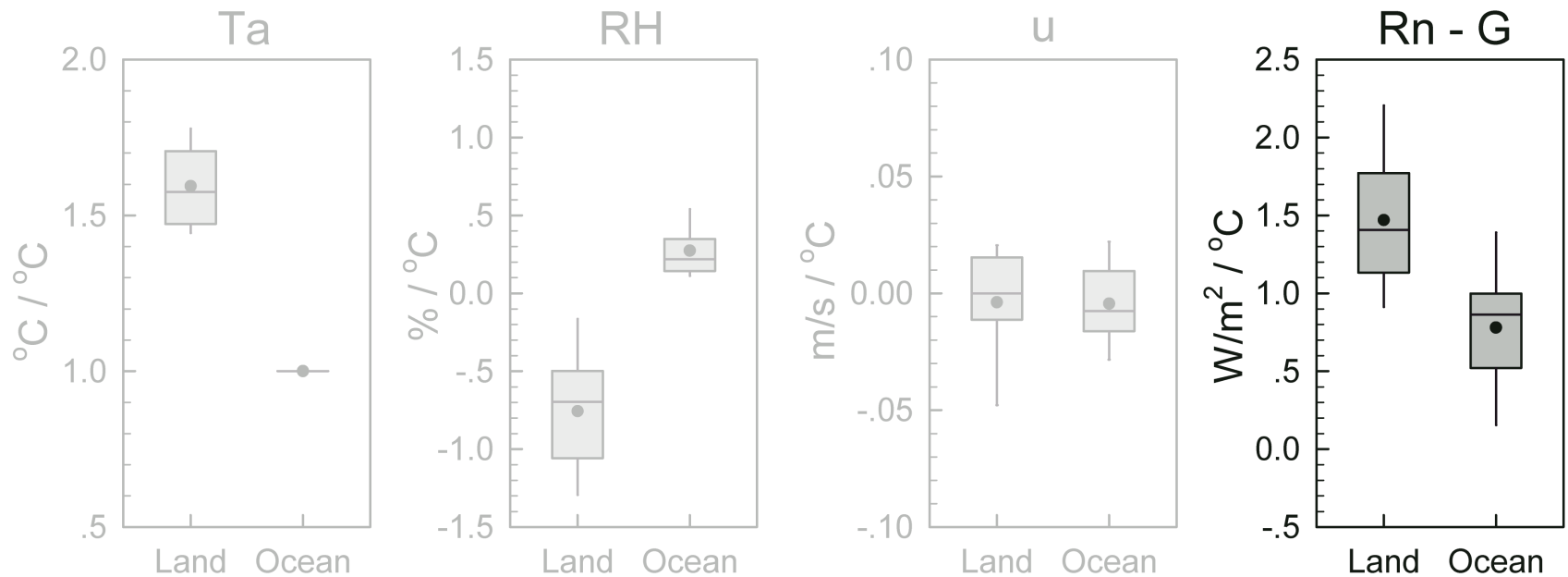
- The surface winds change little over both land and ocean.



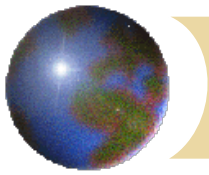
Fu & Feng (2014)



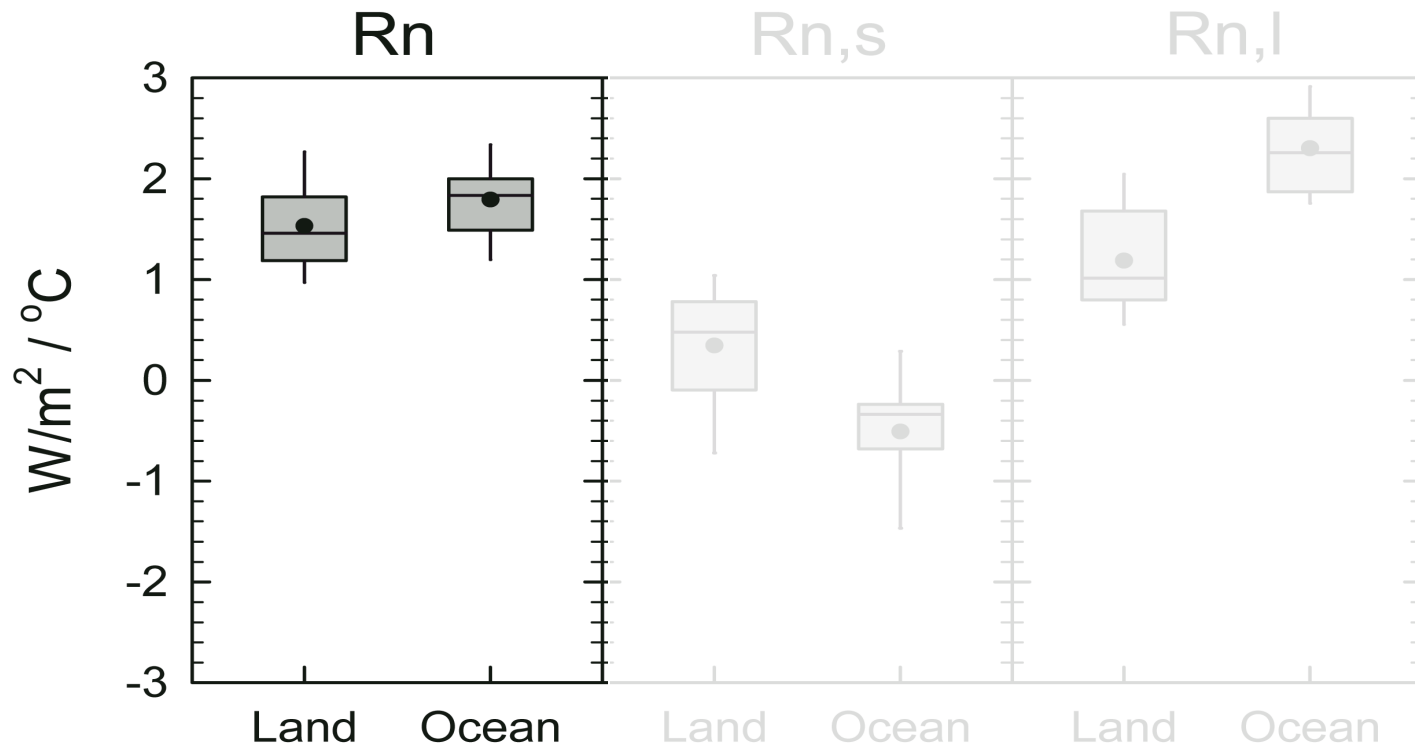
- Ingredient three: Part of increased net downward radiation is transported to deep ocean (e.g., Hansen et al. 2005; Johnson et al. 2011; Loeb et al. 2012)



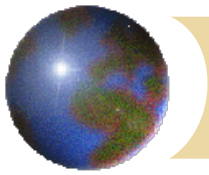
Fu & Feng (2014)



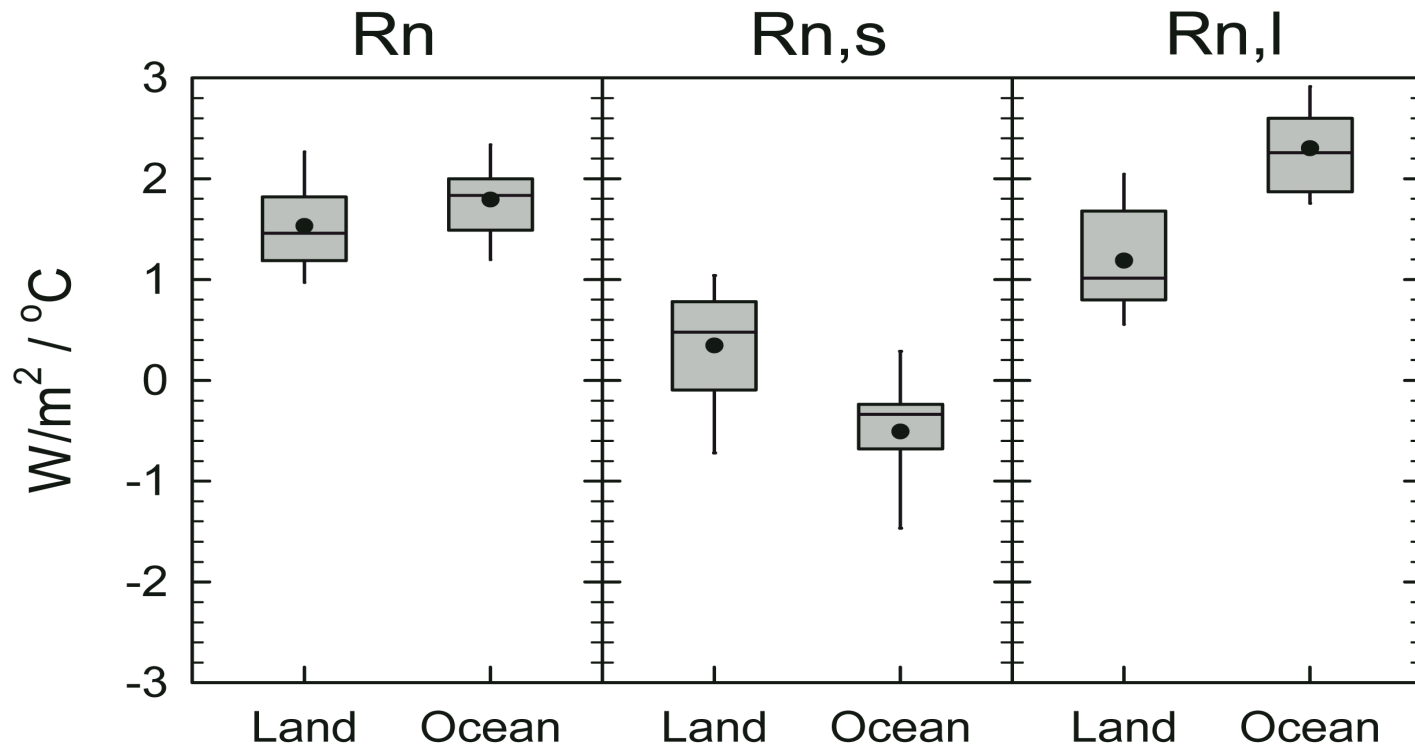
- Change of net radiative energy budget at the surface



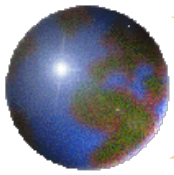
Fu & Feng (2014)



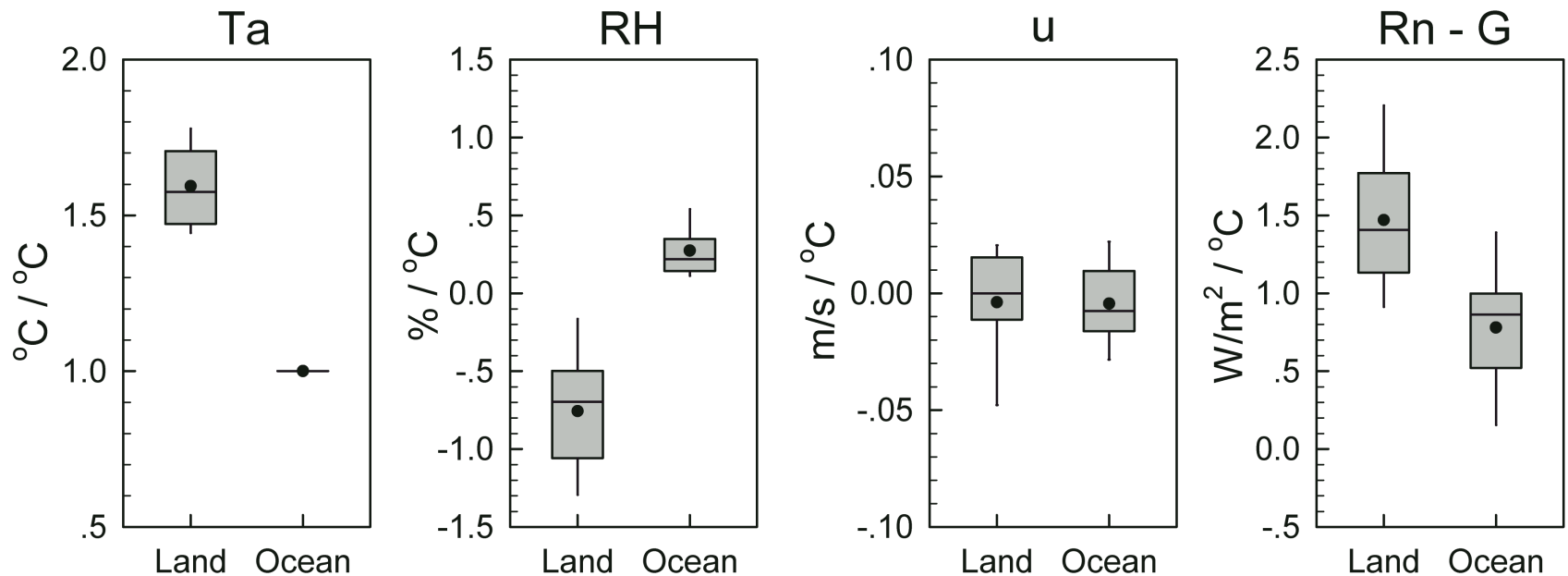
- Change of net radiative energy budget at the surface



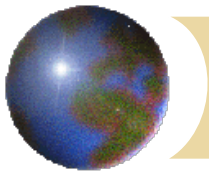
Fu & Feng (2014)



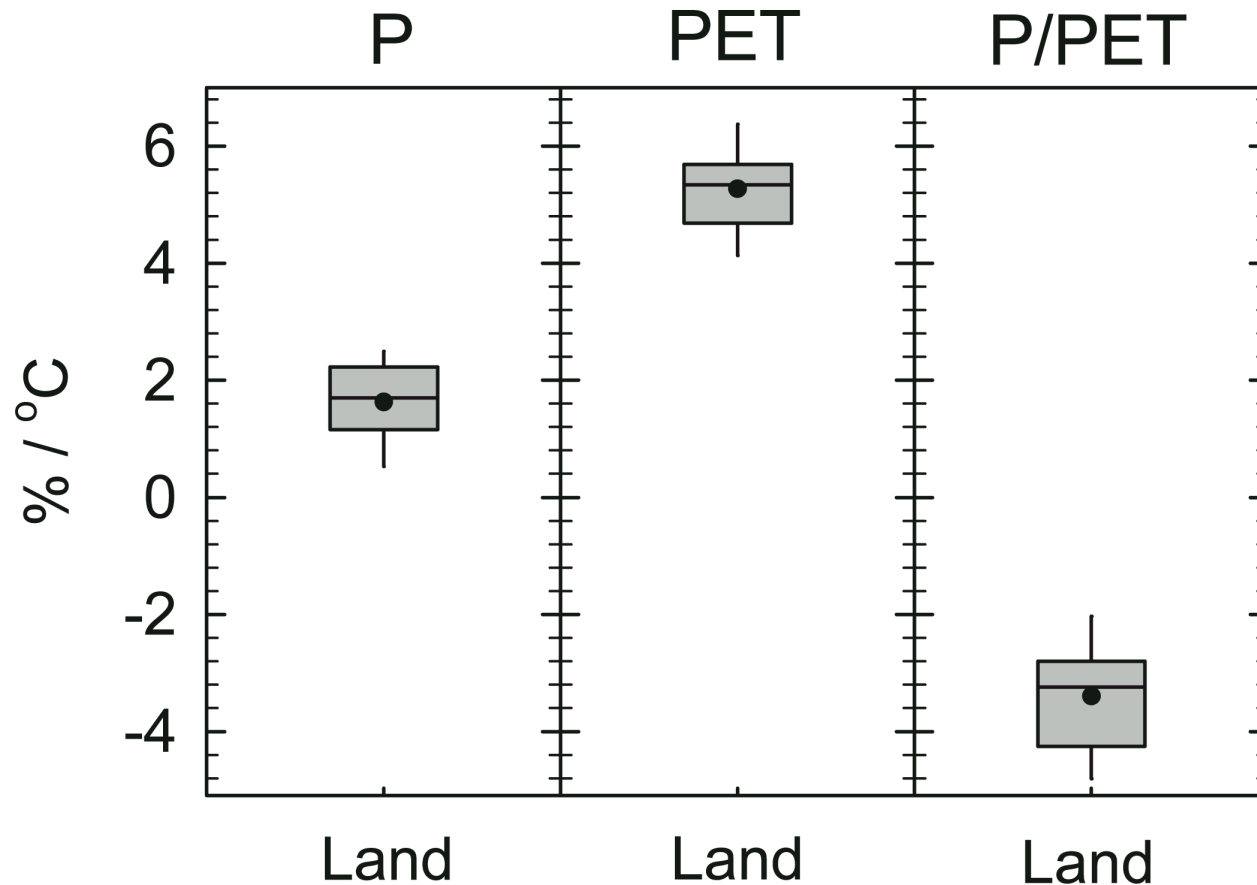
- Ingredients that contribute to a drier terrestrial climate in a warming world



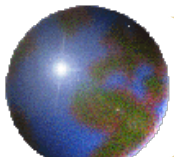
Fu and Feng (2014)



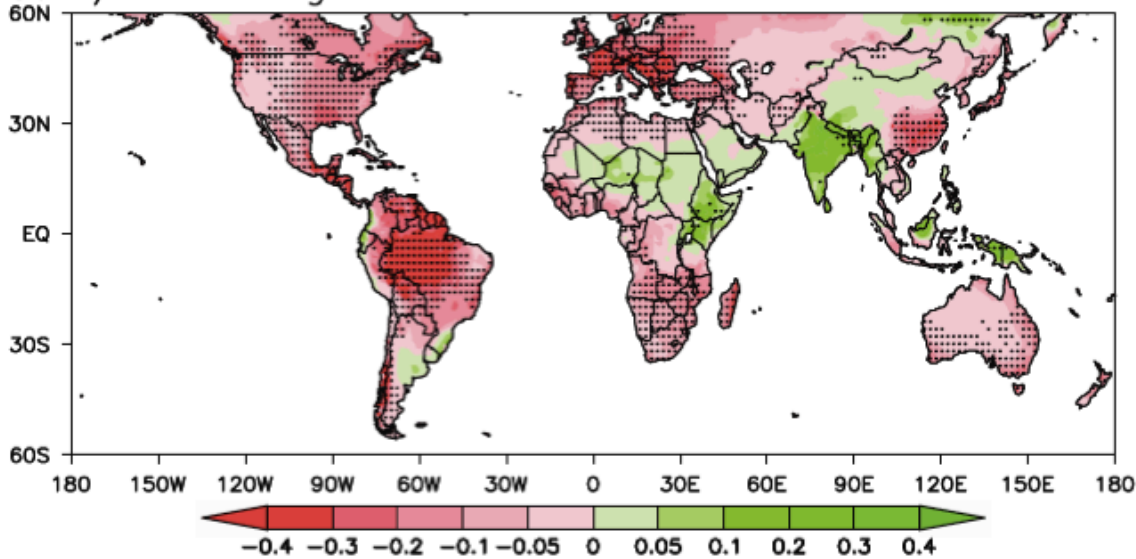
- Our scale analysis shows an averaged decrease of  $P/PET$  by  $\sim 3.4\%/K$  over land



Fu & Feng  
(2014)

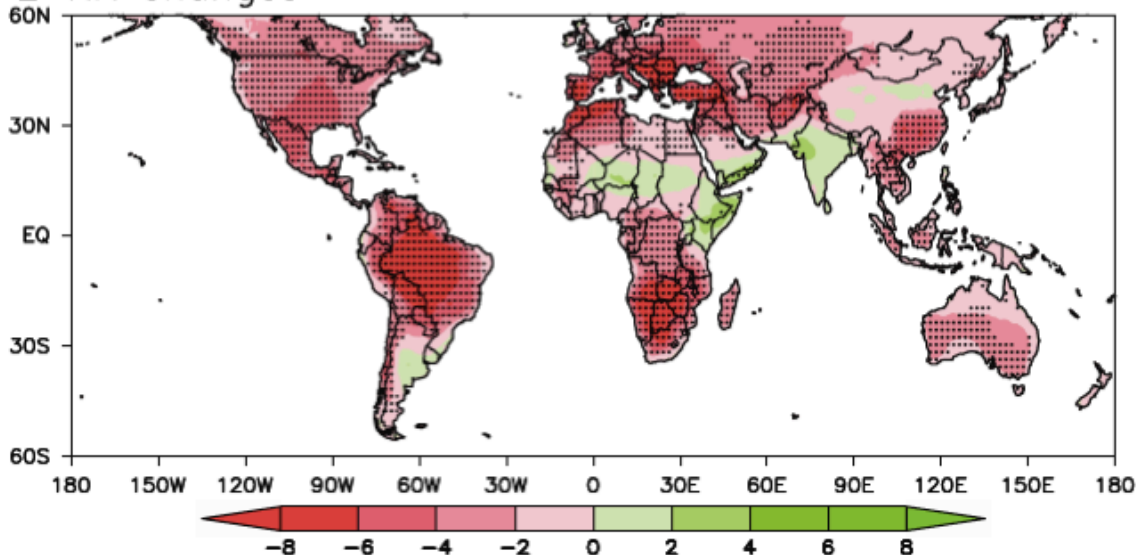


### A P/PET changes



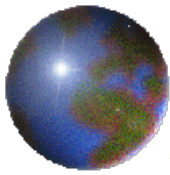
Changes in (a)  $P/PET$  and (b)  $RH$  (1980-1999 to 2080-2099) under scenario RCP85

### B RH changes

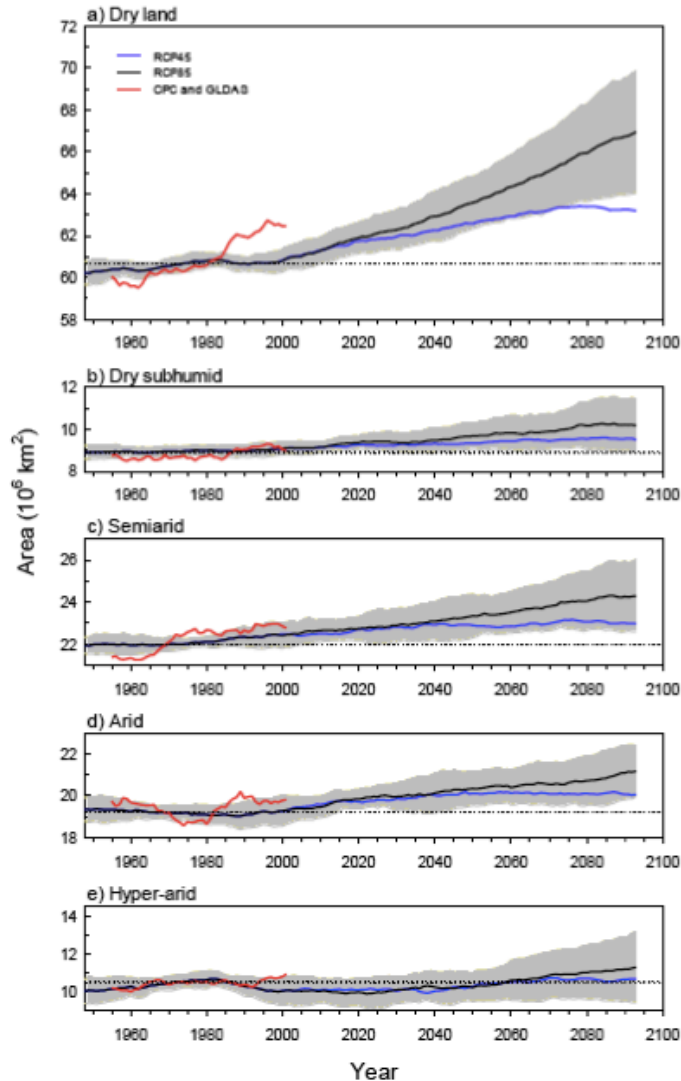


Sherwood & Fu (2014)



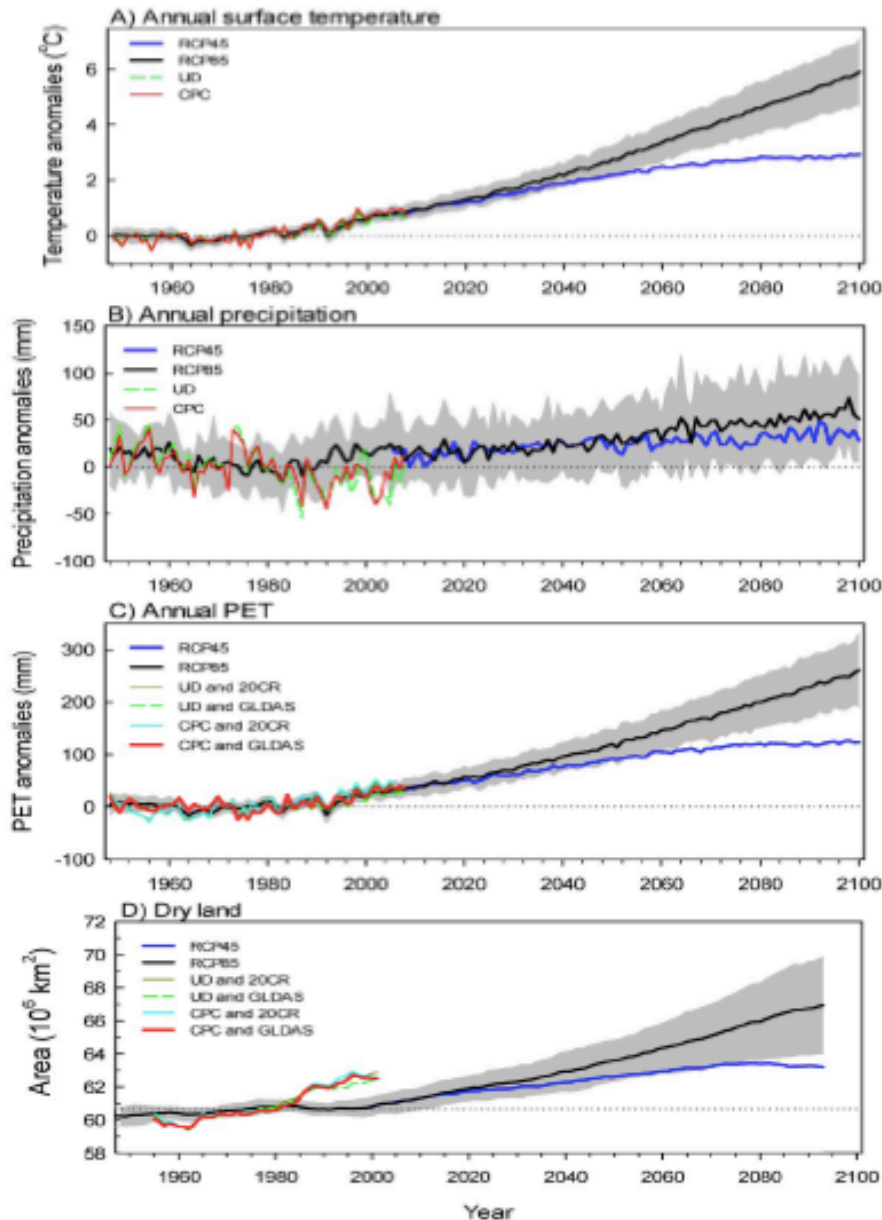
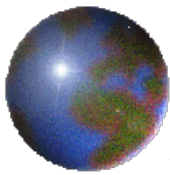


# Global dryland expansion



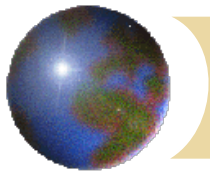
Temporal variations of global dryland areas for (a) the total and individual components of (b) dry subhumid, (c) semiarid, (d) arid, and (e) hyper-arid regions.

Feng and Fu (2013)

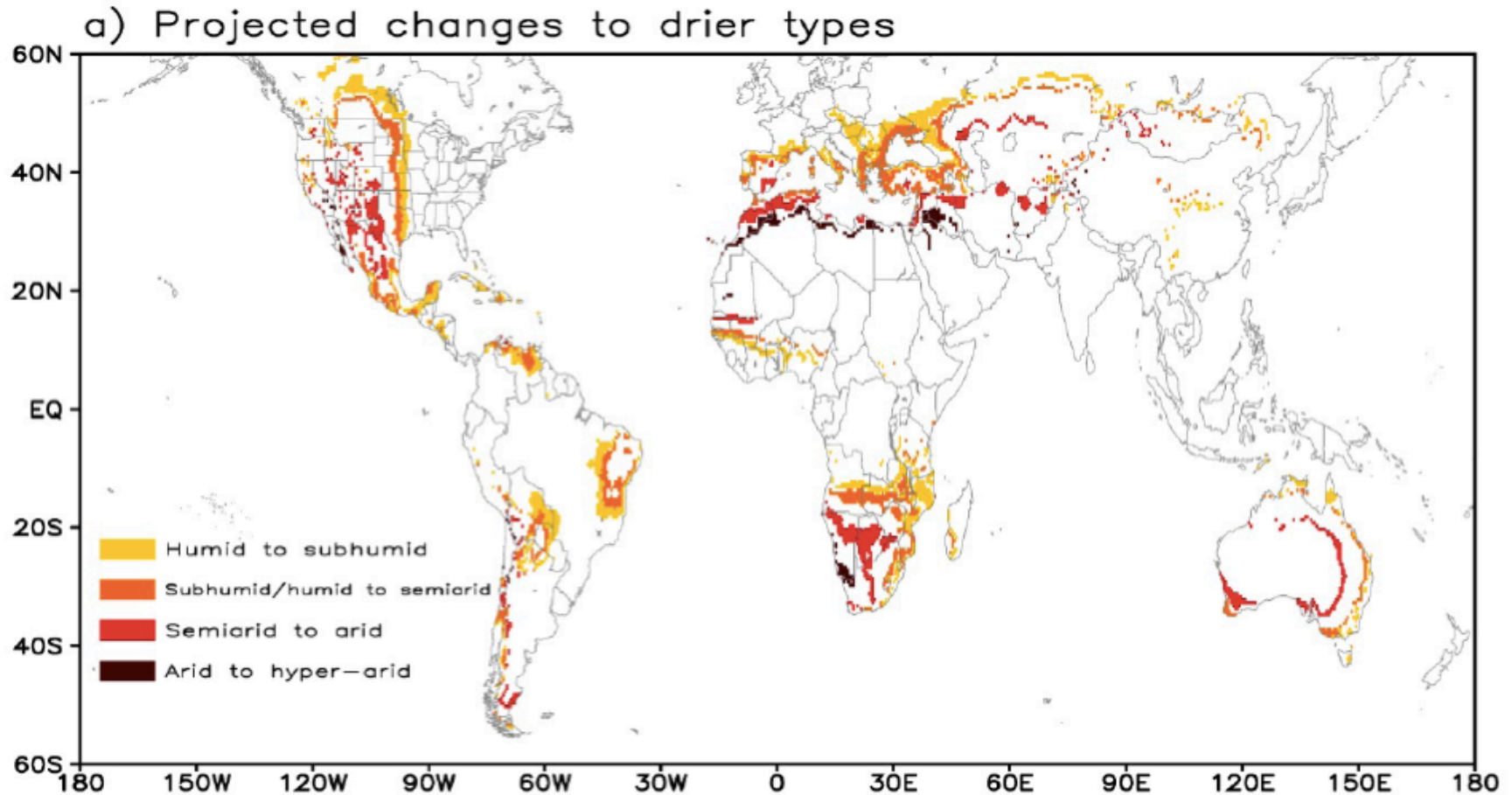


Temporal variations of annual mean (a) surface air temperature, (b) precipitation, and (c) *PET*, averaged over land between 60°N and 60°S, and (d) total area of global drylands.

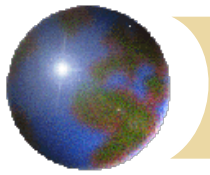
Feng and Fu (2013)



Changes in dryland coverage to drier types (1961-1990 to 2071-2100) under scenario RCP8.5

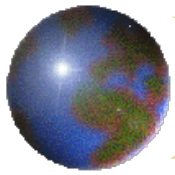


Feng and Fu (2013)



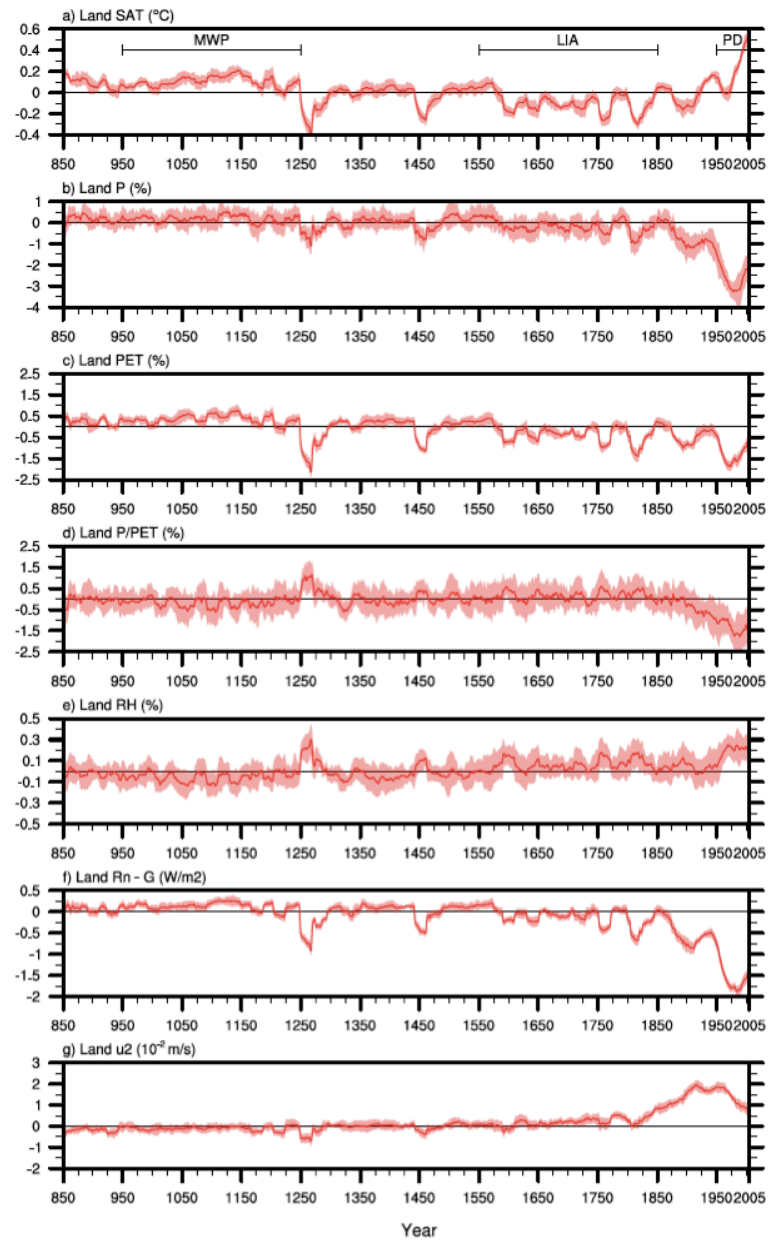
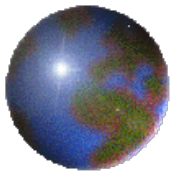
## • Conclusions (I)

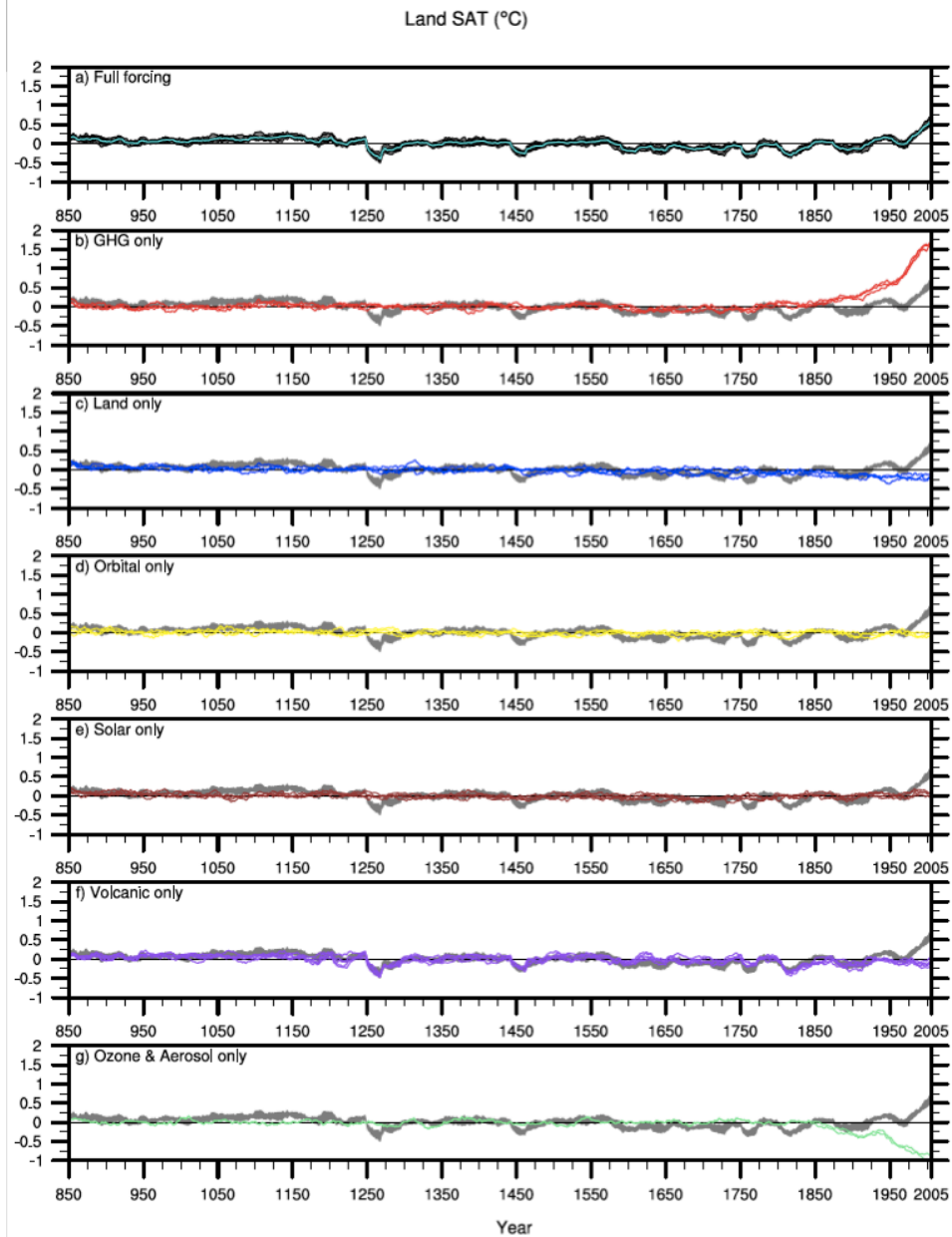
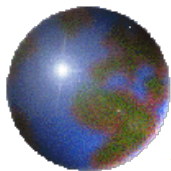
- The climate over land will become drier in a warming world.
- The change in the evaporation over ocean is slower than the change in potential evapotranspiration over land, which leads to a drier terrestrial climate in the future.
- By the end of this century, the world's drylands can be  $5.8 \times 10^6 \text{ km}^2$  (or 10 %) larger than in the 1961–1990 climatology.

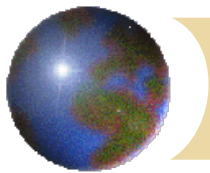


## • Past, present, future

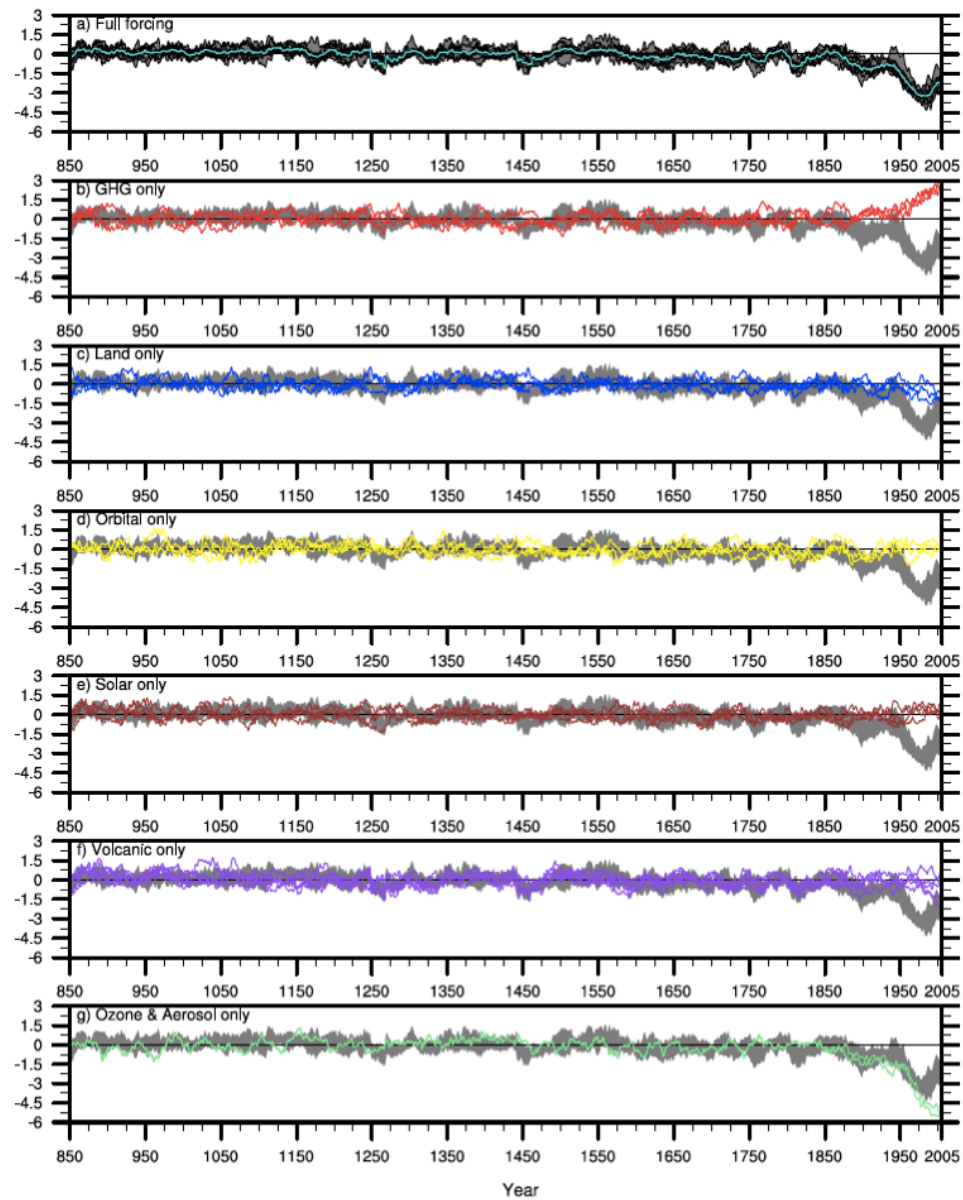
- CESM-LME simulations for 850-2005 (Otto-Bliesner et al. 2015) and CESM-LE for 1920-2080 (Kay et al. 2014)
- Simulations forced with the transient evolution of solar intensity, volcanic emissions, greenhouse gases, aerosols, land use conditions, and orbital parameters, both together and individually.
- to place anthropogenic changes in the context of changes due to natural forcings during last millennium



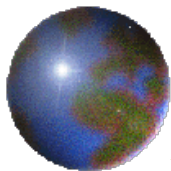




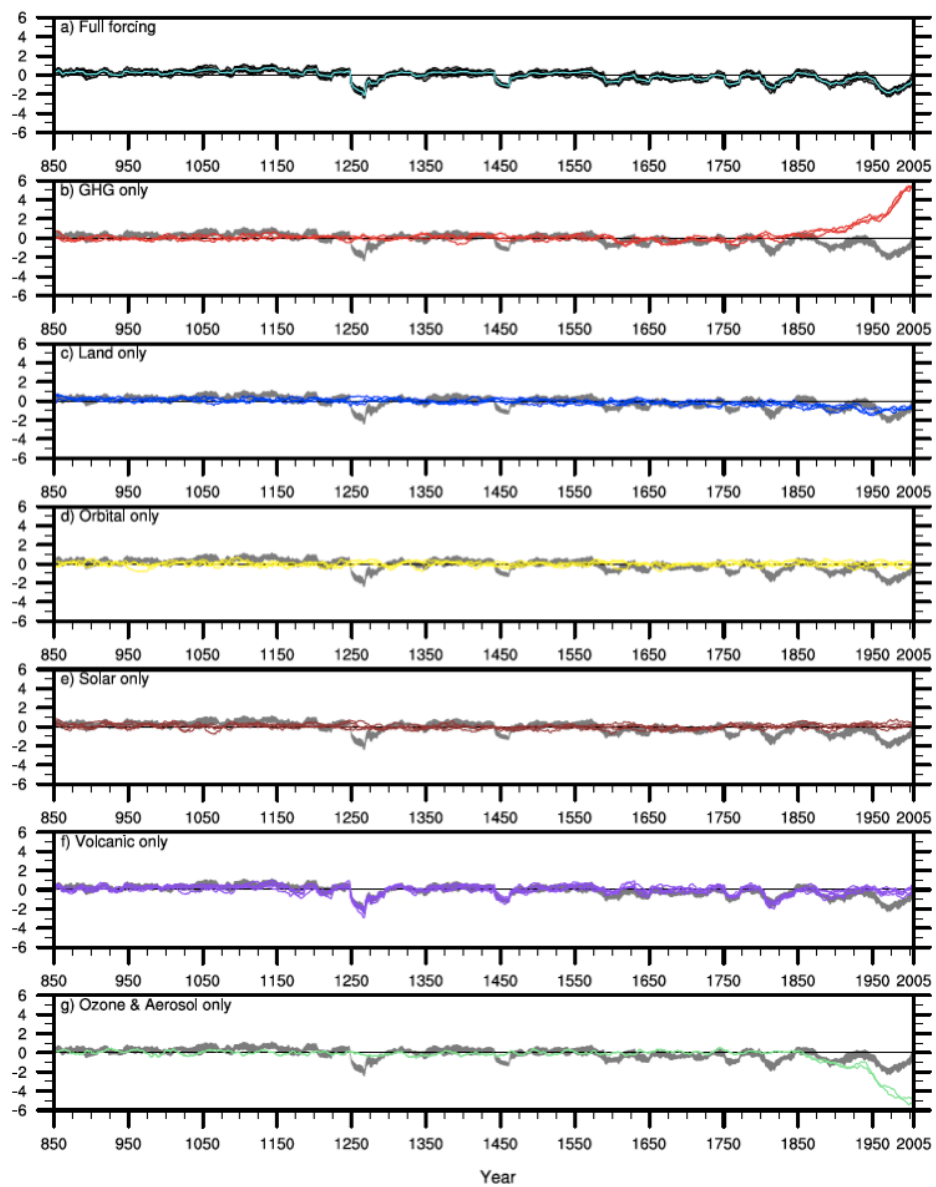
Land P (%)

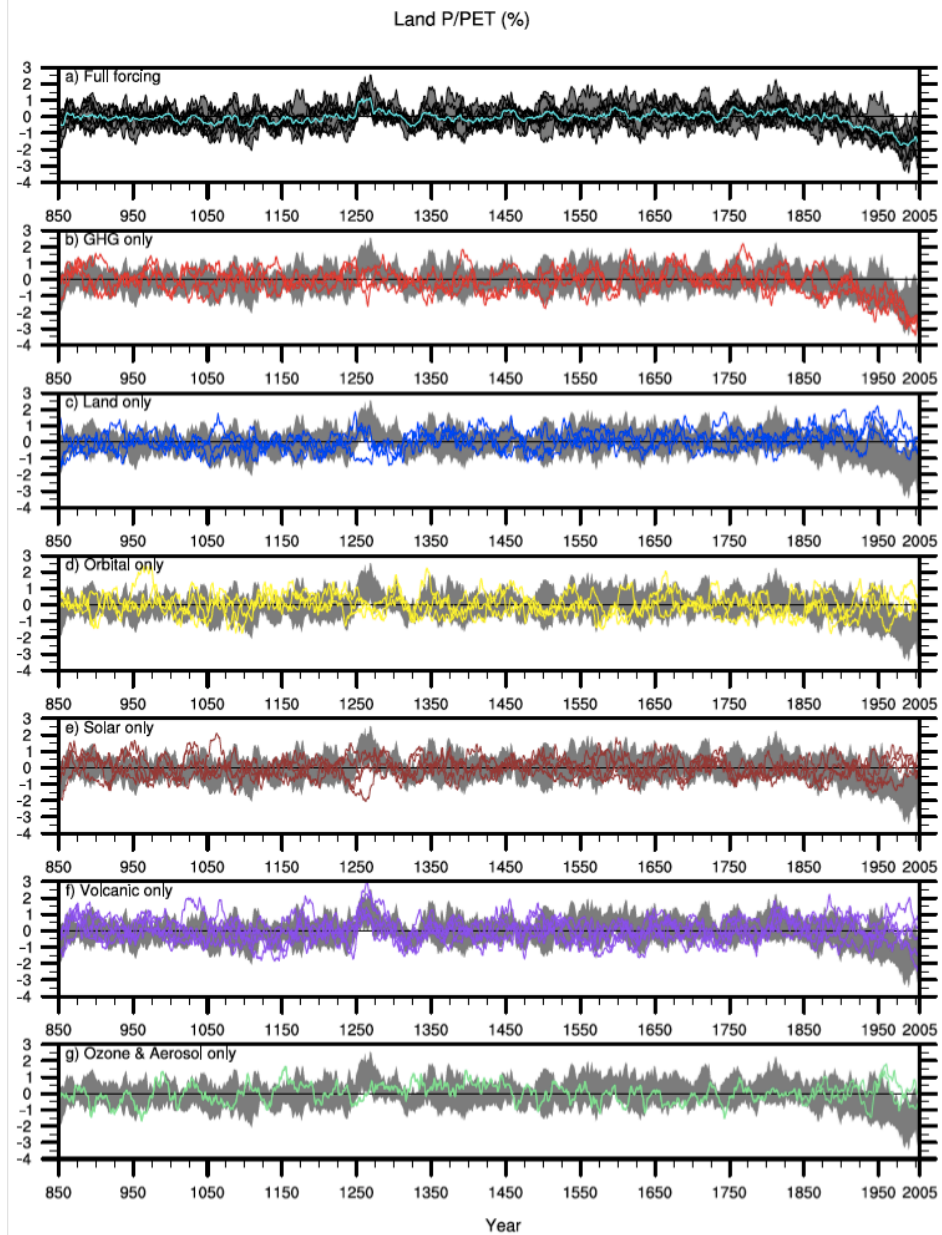
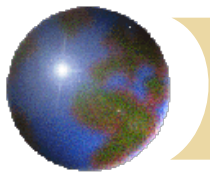


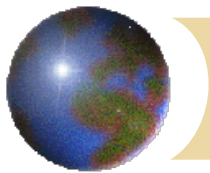




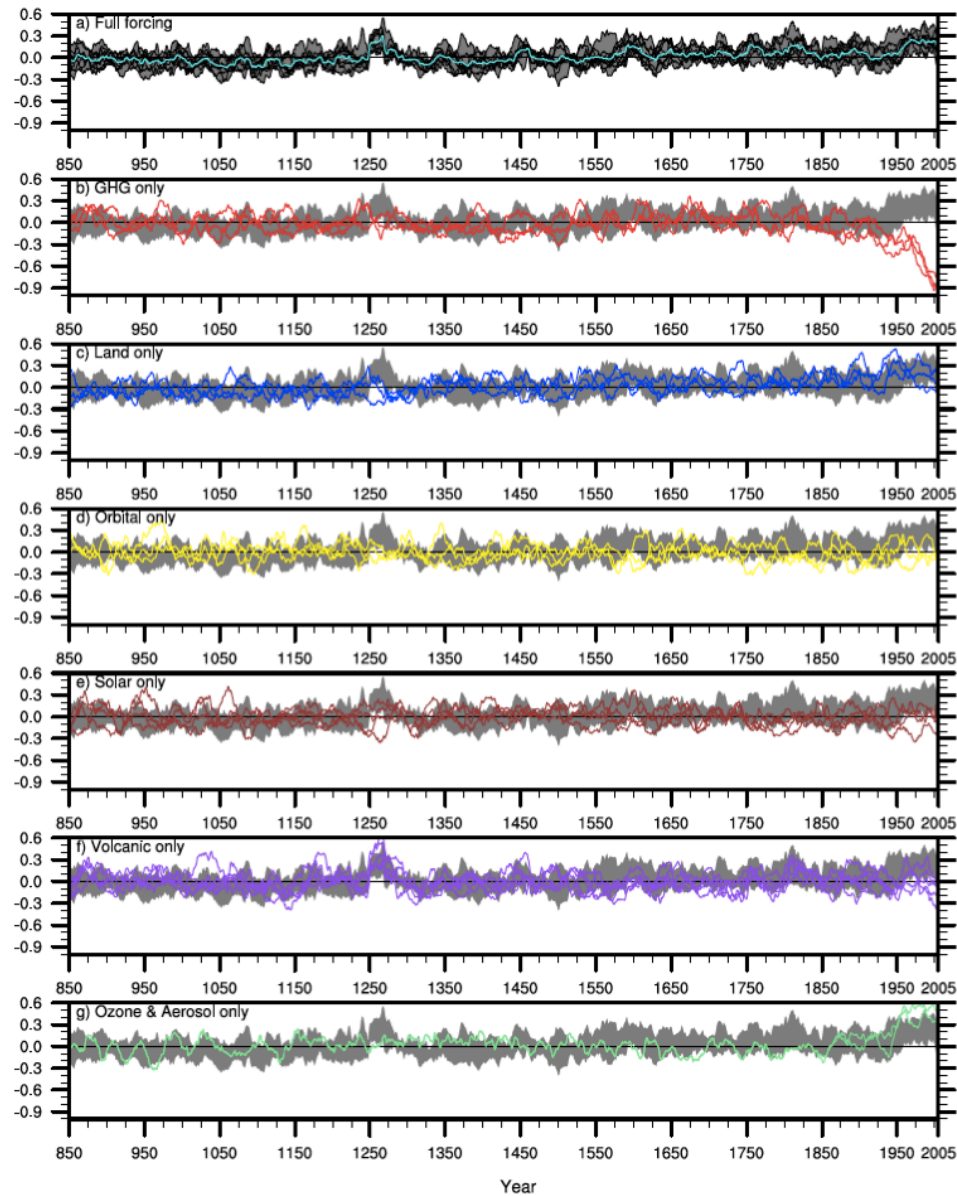
Land PET (%)

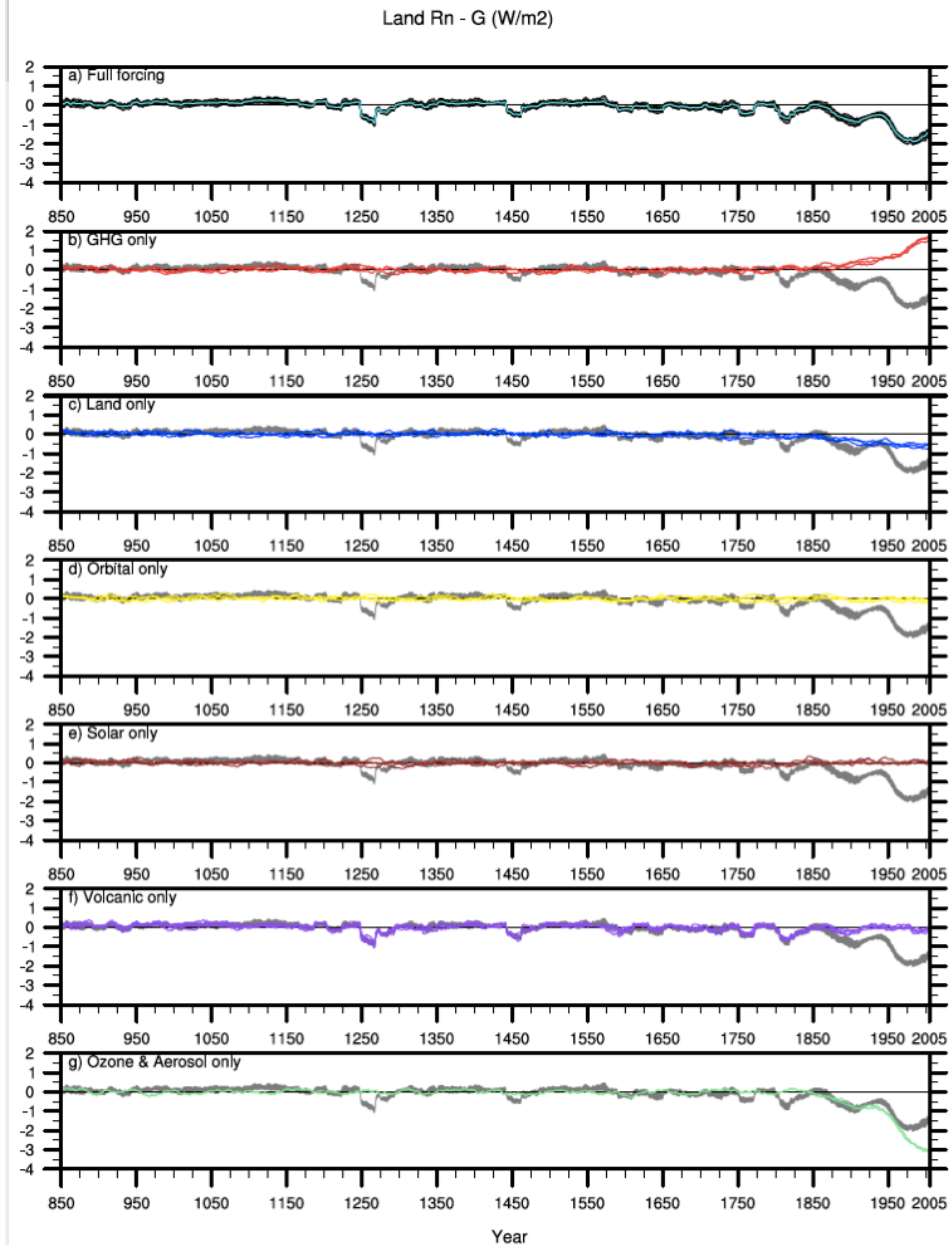
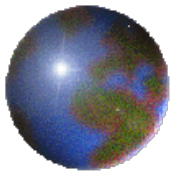


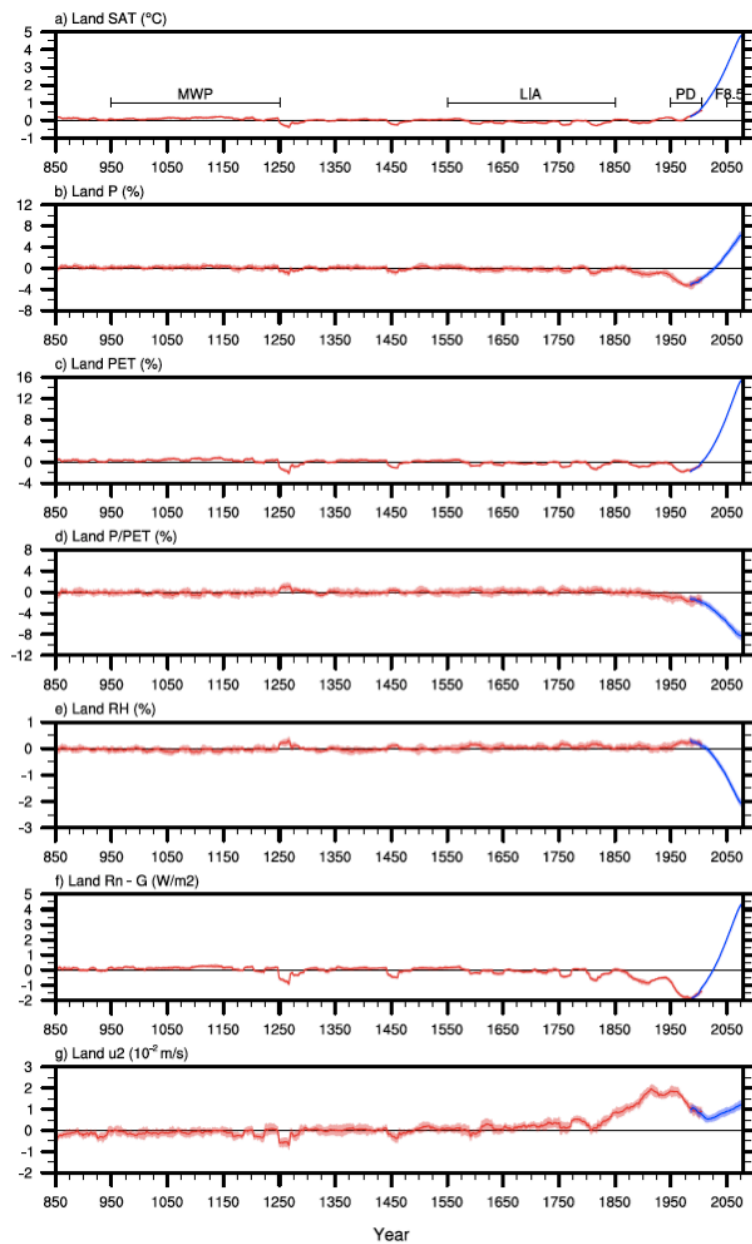
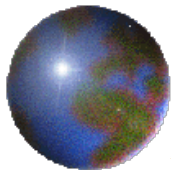


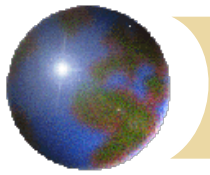


Land RH (%)



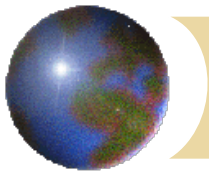






## • Conclusions (II)

- The aridity index averaged over land, becomes smaller (i.e., a drier terrestrial climate) by 0.34% for MWP versus LIA, 1.4% for PD versus LM, and 7.4% for F8.5 versus LM.
- The terrestrial aridity change in PD-LM is largely driven by greenhouse gas increases. Despite small effects on terrestrial-mean aridity, anthropogenic aerosols totally alter the attributions of aridity changes to meteorological variables by causing large negative anomalies in surface air temperature, available energy, and precipitation.
- This study indicates that geoengineering through solar radiation management could not address the problem of a drier climate caused by greenhouse gas increases.



- The PM algorithm was derived from the standard bulk formula for the sensible heat ( $SH$ ) and latent heat ( $LH$ ) fluxes along with the surface energy budget equation

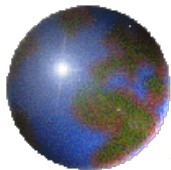
$$SH = \rho_a c_p C_H (T_s - T_a) |u|$$

$$LH = \rho_a L_v C_H (q^*(T_s) - q^*(T_a) RH) |u| / (1 + r_s C_H |u|)$$

$$R_n - G = SH + LH$$

where  $T_s$  is the temperature at the surface interface,  $LH = PET^* L_v$ , and  $q^*$  is the saturated water vapor mixing ratio.





Land U2 (m/s)

